ICAM

Institute for Computational and Applied Mechanics

VARIATIONAL METHODS IN DESIGN OPTIMIZATION AND SENSITIVITY ANALYSIS FOR TWO-DIMENSIONAL EULER EQUATIONS

By

A. H. Ibrahim, S.N. Tiwari, and R. E. Smith
Department of Mechanical Engineering
Old Dominion University, Norfolk, VA 23529

NASA Cooperative Agreement NCC1-232 (S. N. Tiwari, P.I.)
NASA Langley Research Center
Hampton, VA 23665-5225

ODU/ICAM Report 97-102
April 1997

VARIATIONAL METHODS IN DESIGN OPTIMIZATION AND SENSITIVITY ANALYSIS FOR TWO-DIMENSIONAL EULER EQUATIONS

A. H. Ibrahim[1], S. N. Tiwari[2] and R. E. Smith[3]
Old Dominion University

ABSTRACT

Variational methods (VM) sensitivity analysis employed to derive the costate (adjoint) equations, the transversality conditions, and the functional sensitivity derivatives. In the derivation of the sensitivity equations, the variational methods use the generalized calculus of variations, in which the variable boundary is considered as the design function. The converged solution of the state equations together with the converged solution of the costate equations are integrated along the domain boundary to uniquely determine the functional sensitivity derivatives with respect to the design function.

The application of the variational methods to aerodynamic shape optimization problems is demonstrated for internal flow problems at supersonic Mach number range. The study shows, that while maintaining the accuracy of the functional sensitivity derivatives within the reasonable range for engineering prediction purposes, the variational methods show a substantial gain in computational efficiency, i.e., computer time and memory, when compared with the finite difference sensitivity analysis.

---

[1]Research Associate, Department of Mechanical Engineering
[2]Eminent Professor, Department of Mechanical Engineering; AIAA Associate Fellow.
[3]Senior Research Scientist, NASA Langley Research Center; AIAA Associate Fellow.

Forward

This is a report on the research project "Design Optimization and Sensitivity Analysis for Aerodynamic Configurations." This work was conducted as part of the research activities of the Institute for Computational and Applied Mechanics (ICAM) which is now a subprogram of the Institute for Scientific and Educational Technology (ISET). Within the guidelines of the research project, special attention was directed to "Variational Methods in Design Optimization and Sensitivity Analysis for Two-Dimensional Euler Equations." The period of performance of the specific research ended December 31, 1996.

This work, in part, was supported by the NASA Langley Research Center through Cooperative Agreement NCC1-232. The cooperative agreement was monitored by Mr. Roger A. Hathaway, University Affairs Officer, Office of Education, NASA Langley Research Center, Mail Stop 400.

TABLE OF CONTENTS

LIST OF TABLES

LIST OF FIGURES

LIST OF SYMBOLS

A, B	Jacobian matrices in the Cartesian coordinate system
$\overline{A}$, $\overline{B}$	Jacobian matrices in deformed space
$\hat{A}$, $\hat{B}$	Jacobian matrices in the generalized coordinate system
$\hat{A}^{\pm}$, $\hat{B}^{\pm}$	split Jacobians in generalized coordinate system
ADI	alternate directional implicit factorization
$B_{i,n}$	Bezier blending function
$C(n,i)$	binomial coefficients
CFL	Courant-Friedrichs-Lewy number
D	objective function
E, F	inviscid flux components in Cartesian coordinates
$\overline{E}$, $\overline{F}$	nviscid flux components in deformed space
$\hat{E}$, $\hat{F}$	inviscid fluxe vectors in the generalized coordinate system
$\vec{f}$	Bezier generalized function
g_j	constraint functions
G	constraint functional
H, $\overline{H}$	boundary conditions
I	identity matrix
J	functionals or performance indices
$J_{a\Gamma}$	modified functional
J_s	space transformation Jacobian
L	nozzle length
$\hat{n}$	unit vector in deformed spac
nconf	number of generic fluid type constraints
ndv	number of design variables
n_x, n_y	unit vector components in the x and y directions
P	pressure

$\vec{Q}$	conservative variables in undeformed space
$\bar{\vec{Q}}$	conservative variables in deformed space
R	discrete residual in Cartesian coordinate system
$\overline{R}$	continuous residual in Cartesian coordinate system
R_λ	costate residual
S	cross-sectional area
$\vec{S}$	search direction
u	velocity in the x direction
$\overline{u}$	normalized Bezier curve
v	velocity in the y direction
VM	variational methods
$\vec{X}$	spatial vector in the Cartesian coordinates
$\vec{X}_D$	vector of design variables

Greek symbols:

α	move parameter or step size for the search direction
γ	gas constant = 1.4
$\vec{\Gamma}$	vector of boundary components
δ	difference operator
δ	variational symbol
Δ	increment
ε	step size for search direction
η , ξ	generalized curvilinear coordinate components
κ	curvature
$\vec{\lambda}$	vector of Lagrangian parameters
$\vec{\mu}$	vector of constant Lagrangian parameters
$\vec{v}$	vector of extremizing functions
$\vec{v}^*$	vector of optimal extremizing functions

ρ	density
Ω	domain of integration in undeformed space
$\overline{\Omega}$	domain of integration in deformed space

Subscripts:

a	augmented value
i ,j	spatial indices
x , y	Cartesian coordinate components
t	time derivative in Cartesian system
τ	time derivative in generalized curvilinear system
Γ	on the boundary
∞	reference values

Superscripts:

n	temporal level
T	transpose
$\pm$	positive and negative fluxes and Jacobians
*	optimum solutions; intermediate solutions

Special symbols:

$\lvert\ \rvert$	absolute value
$\in$	inclusion or subdomain
$\otimes$	vector multiplication
$\circ$	inner or dot product
∂	partial derivatives

1. INTRODUCTION

1.1 Overview of Aerodynamic Design Optimization and Sensitivity Analysis

In the early times of flight, improvement of vehicle performance was mostly based first on intuition, empirically accumulated databases, and cut-and-try procedures [1,2]. Even recently, wind tunnel testing is being employed to perform optimization work to obtain airfoil performance criteria[3]. While this approach gave many valuable technical assistances, it was unable to furnish quick and reliable information to perform on-line design changes.

In recent years, aerodynamic performance has been analyzed by a method of mathematical optimization. Eventhough there are many ways of optimization, we concenatrate only on the methods of optimization that require gradient information.

1.1.1 Gradient-Based Methods (Numerical Design Optimization)

With the advantage of modern hardware and software computer technologies, numerical design optimization and sensitivity analysis are currently being used to investigate the complete aircraft design problem using two-dimensional Navier-Stokes and three-dimensional Euler equations. These techniques are discussed here briefly.

1.1.1.1 Finite Difference Sensitivity Analysis The simplest, but the most expensive, sensitivity analysis technique used by gradient-based optimization methods is the finite difference approach. This method uses the one-sided or central-difference alternative to evaluate the sensitivities of performance functionals, and consequently, the computational time invested would increase with the increment of the number of design variables. This is due to the requirement to perturb each design variable by an appropriate step size and then compute the flow field variable for each new perturbed design variable with the chosen flow solver. This approach has an additional problem to determine the correct step size *a priori* so that the correct gradient is predicted within a given degree of accuracy. Despite its shortcomings, Huddelston and Mastin [4], and others, have applied this approach in their design procedure with Euler and Navier-Stokes equations. In the

optimization package for general purposes optimizations, Vanderplaats [5] has also incorporated finite difference as an alternative to acquire the gradient information.

1.1.1.2 Discrete Sensitivity Analysis The other category of sensitivity analysis technique is the discrete analysis approach. The computation of the sensitivity equations is based on the Implicit Function Theorem. Due to the implicit dependence of the functional (objective function) and constraints on the flow field quantities, the determination of the sensitivity derivatives is related to obtaining the derivatives of the flow field vector with respect to the design variables. As the flow field equations are in most cases solved in a computational domain, the functional dependence of the metric terms and the coordinate points with respect to the design variables are also required. This approach first calls upon the multiplication and assembly of various terms to a very large sparse linear algebraic equations, which depend on the number of design variables, and then solution of these sparse system of algebraic equations for the derivatives of the solution vector with respect to the design variables. Despite the large computational intensity and huge memory requirements of this approach, the versatility to incorporate many types of constraints, the need to perform multidisciplinary designs of moderate geometrical complexity, and the flexibility to incorporate it with any existing optimization algorithm make it attractive to perform design and shape optimizations.

A wealth of literature can be found for this category. Hicks [6] and Vanderplaats [7,8] have used the discrete approach to design airfoils in transonic flow regimes. Pittman [9] has also used this procedure for supersonic flow conditions. Using the small perturbation equations in two dimensional flows, Elbana and Carlson [10] have also employed the technique. Eleshaky [11] used this method for both internal and external flow problems. He also integrated the domain decomposition method in solving the sensitivity equations. Burgreen [12] further extended the methodology to the three-dimensional wing optimization and introduced an efficient way of parameterizing the curves and surfaces using the Bezier polynomials. With a variant of approximation to the fluid flow, Taylor et al. [13], Newman et al. [14], and Hou et al. [15] introduced an incremental iterative technique to obtain the gradient information. In doing so,

they have applied this new approach not only to the two-dimensional Euler and thin-layer Navier-Stokes turbulent equations for internal and external flows but also to the three-dimensional Euler equations in supersonic flow regimes.

1.1.1.3 Variational Sensitivity Analysis The new emerging sensitivity analysis technique for gradient-based optimization methodology within the optimization community is the continuous sensitivity (variational sensitivity) analysis which fully exploits the variational methods. From the modified functional, this approach derives a set of partial differential equations (PDEs), i.e. the costate equations with their boundary conditions and the sensitivity equations. In computing the sensitivity derivatives with respect to the control points or design variables, this approach makes use of the converged solution of the state and costate equations.

In recent years, variational sensitivity analysis has significantly contributed to the progress of aerodynamic design optimization. Pironneau [16] showed the usefulness of the variational approach in fluid mechanical problems by illustrating how to compute the minimum drag profile in two-dimensional viscous and laminar flows. Chen and Seinfeld [17) developed a methodology to compute the performance sensitivity derivatives using optimal control theory. Koda et al. [18] used this procedure to solve atmospheric diffusion problems. Koda [19 - 21] further developed this approach and outlined a numerical algorithm for the computation of functional derivatives. This approach is well suited to solving the optimum design problems in fluid mechanics. Meric [22,23] treated optimal control problems governed by parabolic and elliptic partial differential equations and solved them numerically using variational methods. In their effort to compare the gradients obtained by "implicit" and "variational" approaches, Shubin and Frank [24] implemented VM to optimize the shape of a nozzle of a variable cross - sectional area for steady one-dimensional Euler equations. Jameson [25] regarded the boundary of the flow domain as a control parameter and then designed airfoils using the potential as well as the two- and three-dimensional compressible inviscid flows. Cabuk and Modi [26] implemented a perturbation method to compute the optimum profile of a diffuser for a maximum static pressure in a two-dimensional steady viscous incompressible flow. Ta'asan et al. [27] have successfully

implemented variational methods and optimized an airfoil in the potential flow field. Quite recently, Ibrahim and Baysal [28] demonstrated the versatility of the variational methods to solve aerodynamical design problems for internal flows in different Mach number regimes including shock flows. Following the same approach as Jamson [25], Reuter and Jameson [29] optimized airfoils in potential flows. Iollo and Salas [30] used variational methods to solve two-dimensional internal flow optimization problem with embedded shock to match a pressure distribution. In this class of optimization, the functional sensitivity derivatives are directly coupled to the solution of a set of linear partial differential equations, i.e., the costate equations and their boundary or transversality conditions that result from the variation of the augmented Lagrangian function. The success of any optimization by this approach is, therefore, destined to a stable and converged solution of the costate equations.

1.2 Generality of the Variational Approach

First, since the costate equations are once and for all derived from the continuous PDE of the state equation, any robust solution method can be adopted to furnish the converged solution so that the costate equations can be solved until convergence is attained. This means that one does not necessarily have to solve the original state equation from which the costate equations are derived. Secondly, any other convenient discretization methods different from the type of discretization one uses for the state equations can be selected for the costate equations. The requirement that the costate equations be discretized exactly the same way as the state equations is shown not to be necessary, at least for quasi one-dimensional Euler equations [31]. Thirdly, any time integration method different from the time integration method used for the state equation can be selected to advance the costate equations to steady state. The fourth point to mention is the design variables. In the approach proposed, note that the shape of the domain is considered as the design parameter, and its contribution to the functional sensitivity derivatives is directly incorporated as shown in Ref. 32.

2. AERODYNAMIC DESIGN OPTIMIZATION AND SENSITIVITY ANALYSIS

2.1 Constrained Optimization Methodology

A constrained optimization method in general encompasses three elements of optimization, i.e., design variables, constraints, and objective function. These are discussed here briefly.

2.1.1 Design Variables in Variational Sense

In most aerodynamic optimization problems, the design variables are generally of a geometric nature, such as the coefficients of some geometric functions, surface grid points [11], aerofunctions [33], or polynomial functions such as Bezier-Bernstein functions [12,34] and spline functions [35].

Variational methods treat the boundary of the domain in a continuous fashion, and therefore, the boundary is considered as part of the solution to the design problem. With the assumption that the domain Ω is sufficiently regular, the location of points on the boundary $\vec{X}_\Gamma$ can be considered as a continuous design variable. Mathematically, the coordinates of the varying boundary in the continuous sense can be expressed as

$$\vec{X}_\Gamma = \vec{f}(\vec{X}_D) \tag{1}$$

where $\vec{X}_d$ are the design variables. In aerodynamic optimization problems, the vector of design variables is provided for very limited and simplified geometries, for instance, four digit NACA airfoils and some nozzles. However, for general-purpose geometries, these control points must be determined through iterative methods from certain functional relationships such as the Bezier-Bernstein polynomials [12]. Because these polynomial functions are known to generate smooth curves and surfaces for a minimal number of control points, the function $\vec{f}$ which describes the curve for the two-dimensional problem, is given by [34]

$$\vec{f}(\bar{u}) = \sum_{i=0}^{n} \vec{X}_{d,i} B_{i,n}(\bar{u}) \qquad \text{for} \qquad \bar{u} \in [0,1] \qquad (2)$$

where

$$B_{i,n}(\bar{u}) = C(n,i)\bar{u}^{i}(1-\bar{u})^{n-i} \qquad (3)$$

$$C(n,i) = \frac{n!}{i!(n-i)!} \qquad (4)$$

In Eqs. (2) - (4), $B_{i,n}(\bar{u})$ are the blending functions, which are key to the behavior of the curve, $C(n,i)$ are the binomial coefficients, $\bar{u}$ is the normalized arc length and n is the order of the Bezier-Bernsten polynomials. In this study, with the use of Eqs. (1) - (4), the location of the control points can be considred as the design variables.

2.1.2 Constraints

Constraints are the integral parts of the optimization procedure that influence the final outcome of the functional. They can be geometrical, flow-type, equality or inequality constraints, or a combination of all or some that depends on the particular optimization problem one wants to address.

In the variational formulation of design optimization problems, the flow-type constraints are expressed in the integral forms. The geometrical and side constraints, on the other hand, can be formulated either in the integral or discrete forms. For the general variational approach, generic flow-type constraints are expressed as

$$G_j(\vec{Q},\vec{n}) = \int_{\bar{\Gamma}} g_j(\vec{Q},\vec{n}) d\bar{\Gamma} \le 0 \qquad \text{for } j = 1, 2, ..., \text{nconf} \qquad (5)$$

where $\bar{\Gamma}$, is the deformed boundary and nconf is the number of generic fluid-type constraints. The generic geometric-type and the side constraints can also be given as

$$G_j(\vec{X}_D) \le 0 \qquad \text{for } j = \text{nconf+1, nconf+2, ..., ncon} \qquad (6)$$

and

$$X_{iD}^{lower} \le X_{iD} \le X_{iD}^{upper} \qquad \text{for } i = 1, 2, ..., \text{ndv} \qquad (7)$$

where ncon is the total number of constraints, and ndv is the number of design variables, respectively.

2.1.3 Objective Functional

In the variational methods (VM), the objective functional is defined in the form of a definite integral involving an unknown state function $\vec{Q}$, which can be dependent on some normal vectors $\vec{n}$ and other problem parameters. Then, the objective functional is extremized at the converged state solution over the curve of the surface described by the vector of design variables. Mathematically, a generic functional on the boundary $J_{\bar{\Gamma}}$, is defined as

$$J_{\bar{\Gamma}}(\vec{Q},\vec{n}) = \int_{\bar{\Gamma}} D(\vec{Q},\vec{n}) d\bar{\Gamma} \qquad (8)$$

where D, for the two-dimensional problem, is the objective function specified on the curve or boundary. The selection of the objective function is mostly dictated by the flow physics.

2.2 Variational Formulation of Aerodynamic Optimization Problem

When constraints are involved in the optimization problem, the partial derivatives of the functional and the constraints cannot be zero at the same time since they are functionally related to each other through the optimality criteria [36, 37]. One common practice is to cast the constrained optimization to unconstrained optimization through the introduction of the weighting functions or Lagrange multipliers $\vec{\lambda}(\vec{X})$. The other is to sequentially solve a linear or quadratic

programming problem, which is an approximation of the original constained minimization problem. In the later approach, one needs to derive the sensitivities of the performance functional.

To start the derivation, the steady state solution of the two-dimensional Euler equations, i.e., the residual $\overline{R}(\vec{Q})$, is written as

$$\overline{R}(\vec{Q}) = \overline{E}_x + \overline{F}_y = \vec{0} \tag{9}$$

and the generic boundary conditions are expressed as

$$\overline{H}(\vec{Q},\vec{n}) = \vec{0} \tag{10}$$

Without changing its value, the objective functional $J_{\overline{\Gamma}}$ can now be modified as

$$J_{\overline{\Gamma}a}\left(\vec{Q},\vec{n},\vec{\lambda},\vec{\mu}\right) = J_{\overline{\Gamma}} + \int_{\overline{\Omega}} \vec{\lambda}^T(\vec{X})\overline{R}(\vec{Q})d\overline{\Omega} + \int_{\overline{\Gamma}} \vec{\mu}^T\overline{H}(\vec{Q},\vec{n})d\overline{\Gamma} \tag{11}$$

where $\overline{\Gamma}$ and $\overline{\Omega}$ are the deformed boundary and domain, and $\vec{\lambda}$ and $\vec{\mu}$ are vectors to be determined.

2.2.1 Standard Formulation of an Aerodynamic Optimization Problem

A mathematical formulation of the constrained optimization problem can be expressed as

$$\min_{\Gamma} \quad \{J_\Gamma\} \tag{12}$$

subject to

$$G_j(\vec{Q},\vec{n}) = \int_{\overline{\Gamma}} g_j(\vec{Q},\vec{n})d\overline{\Gamma} \le 0 \qquad \text{for } j = 1, 2, ..., \text{nconf} \tag{13}$$

$$G_j(\vec{X}_D) \le 0 \qquad j = \text{nconf+1, nconf+2, ..., ncon} \qquad (14)$$

and

$$X_{iD}^{lower} \le X_{iD} \le X_{iD}^{upper} \qquad i = 1, 2, ..., \text{NDV} \qquad (15)$$

where the flow field variables $\vec{Q}$ are the solution to the state equations, $\overline{R}(\vec{Q})$.

2.2.2 Derivation of Functional Sensitivity Equations

As the detailed derivation for functional sensitivity is showen in Ref. 32, we give here only the high lights of the procedure. Hence, the variation of the fluxes (to the first order) can be written as

$$\delta\overline{E} = \overline{A}\,\delta\vec{Q} \quad \text{and} \quad \delta\overline{F} = \overline{B}\,\delta\vec{Q} \qquad (16)$$

where $\overline{A}$, and $\overline{B}$ are the Jacobian matrices in the x and y directions, respectively. Then the fluxes on the deformed space due to the variation of the boundary can be approximated as

$$\overline{E}(\bar{\vec{Q}}) = \overline{E}(\vec{Q}) + \delta\overline{E}(\vec{Q}) \quad \text{and} \quad \overline{F}(\bar{\vec{Q}}) = \overline{F}(\vec{Q}) + \delta\overline{F}(\vec{Q}) \qquad (17)$$

By application of the principles of calculus of variations, the variation of the modified functional can be approximated by [36]

$$\Delta J_{\Gamma a} = J_{\bar{\Gamma}a}\left(\bar{\vec{Q}}\left(\bar{\vec{X}}\right), \bar{\vec{\lambda}}\left(\bar{\vec{X}}\right), \bar{\vec{\mu}}\left(\bar{\vec{X}}\right)\right) - J_{\Gamma a}\left(\vec{Q}(\vec{X}), \vec{\lambda}(\vec{X}), \vec{\mu}(\vec{X})\right) \qquad (18)$$

where $\bar{\vec{X}}$ and $\vec{X}$ are position vectors of the deformed and undeformed coordinate systems, respectively. Then, the Taylor expansion of the integrand of Eq. (18) is computed (the linear part relative to ε) as [36-38]

$$\delta J_{\Gamma a} = \int_{\Gamma}\left\{D + D_Q\delta\bar{\bar{Q}} + D_n\delta n + D\kappa\delta n\right\}d\Gamma + \int_{\Gamma}(\vec{\mu}^T + \delta\vec{\mu}^T)\left\{\bar{H} + \bar{H}_Q\delta\bar{\bar{Q}} + \bar{H}_n\delta n + \bar{H}\kappa\delta n\right\}d\Gamma$$
$$+ \int_{\Omega}\left\{\left(\vec{\lambda}^T + \delta\vec{\lambda}\right)^T\left[\bar{E}_x(\vec{Q}) + (\delta\bar{E}(\vec{Q}))_x + \bar{F}_y(\vec{Q}) + (\delta\bar{F}(\vec{Q}))_y\right]\right\}|J_S|d\Omega$$
$$- \int_{\Omega}\vec{\lambda}^T\left[\bar{E}_x(\vec{Q}) + \bar{F}_y(\vec{Q})\right]d\Omega - \int_{\Gamma}\left[D + \vec{\mu}^T\bar{H}\right]d\Gamma \qquad (19)$$

where ε is a small parameter, J_s is the space transformations matrix that is given as $|J_S| = \left|I + \vec{\nabla}.\delta\vec{X}\right|$ [32] and the quantity κ in Eq. (19) is the curvature and can be calculated as [37]

$$\kappa = -\vec{\nabla}\circ\vec{n} \qquad (20)$$

where $\circ$ denotess a dot or inner product and $\vec{n}$ is the unit normal which can be computed from the grid generating routine or from the analytical derivatives of the Bezier-Bernstein polynomials as [34]

$$\kappa = \left[\frac{\partial\vec{f}}{\partial\bar{u}}\otimes\frac{\partial^2\vec{f}}{\partial\bar{u}^2}\right]\left\{\left|\frac{\partial\vec{f}}{\partial\bar{u}}\right|^3\right\}^{-1} \qquad (21)$$

where $\otimes$ is a vector multiplication sign and $\vec{f}(\bar{u})$ is defined in Eq. (2). In Eq. (19), δn is defined as

$$\delta n = \delta\vec{X}\circ\vec{n} \qquad (22)$$

Now, by taking only the linear terms of Eq. (19), one obtains

$$\delta J_{\Gamma a} = \int_{\Gamma}\left\{D_Q\delta\bar{\bar{Q}} + D_n\delta n + D\kappa\delta n + \vec{\mu}^T\left[\bar{H}_Q\delta\bar{\bar{Q}} + \bar{H}_n\delta n + \bar{H}\kappa\delta n\right]\right\}d\Gamma$$
$$+ \int_{\Omega}\left\{\vec{\lambda}^T\left[(\delta\bar{E}(\vec{Q}))_x + (\delta\bar{F}(\vec{Q}))_y\right]\right\}d\Omega + \int_{\Omega}\left\{\left(\delta\vec{\lambda}\right)^T\left[\bar{E}_x(\vec{Q}) + \bar{F}_y(\vec{Q})\right]\right\}d\Omega + \int_{\Gamma}\delta\vec{\mu}^T\bar{H}d\Gamma$$
$$+ \int_{\Gamma}\vec{\lambda}^T\left[\bar{E}_x + \bar{F}_y\right]\delta n d\Gamma \qquad (23)$$

Using Eq.(16) and performing integration by parts, the second term in Eq. (23) is expressed as

$$\int_{\Omega}\left\{\vec{\lambda}^T\left[(\delta\overline{E}(\vec{Q}))_x+(\delta\overline{F}(\vec{Q}))_y\right]\right\}d\Omega=\int_{\Omega}\left\{-\vec{\lambda}_x^T\overline{A}-\vec{\lambda}_y^T\overline{B}\right\}\delta\vec{\overline{Q}}\,d\Omega + \int_{\Gamma}\left\{\vec{\lambda}^T\left[\overline{A}n_x+\overline{B}n_y\right]\delta\vec{\overline{Q}}\right\}d\Gamma \tag{24}$$

Substitution of Eq. (24) into Eq. (23) gives

$$\begin{aligned}\delta J_{\Gamma a}=&\int_{\Gamma}\left\{D_Q\delta\vec{\overline{Q}}+D_n\delta n+D\kappa\delta n+\vec{\mu}^T\left[\overline{H}_Q\delta\vec{\overline{Q}}+\overline{H}_n\delta n+\overline{H}\kappa\delta n\right]\right\}d\Gamma\\&+\int_{\Gamma}\left\{\vec{\lambda}^T\left[\overline{A}n_x+\overline{B}n_y\right]\delta\vec{\overline{Q}}\right\}d\Gamma+\int_{\Omega}\left\{-\vec{\lambda}_x^T\overline{A}-\vec{\lambda}_y^T\overline{B}\right\}\delta\vec{\overline{Q}}\,d\Omega\\&+\int_{\Omega}\left\{\left(\delta\vec{\lambda}\right)^T\left[\overline{E}_x(\vec{Q})+\overline{F}_y(\vec{Q})\right]\right\}d\Omega+\int_{\Gamma}\delta\vec{\mu}^T\overline{H}d\Gamma+\int_{\Gamma}\vec{\lambda}^T\left[\overline{E}_x+\overline{F}_y\right]\delta n d\Gamma\end{aligned} \tag{25}$$

Note that for the arbitrary variations of $\delta\vec{\lambda}$ and $\delta\vec{\mu}$ and with Eqs. (9) and (10), the last two terms in Eq. (25) are identically zero. Then Eq. (25) reduces to

$$\begin{aligned}\delta J_{\Gamma a}=&\int_{\Gamma}\left\{D_Q\delta\vec{\overline{Q}}+D_n\delta n+D\kappa\delta n+\vec{\mu}^T\left[\overline{H}_Q\delta\vec{\overline{Q}}+\overline{H}_n\delta n+\overline{H}\kappa\delta n\right]\right\}d\Gamma\\&+\int_{\Gamma}\left\{\vec{\lambda}^T\left[\overline{A}n_x+\overline{B}n_y\right]\delta\vec{\overline{Q}}\right\}d\Gamma+\int_{\Omega}\left\{-\vec{\lambda}_x^T\overline{A}-\vec{\lambda}_y^T\overline{B}\right\}\delta\vec{\overline{Q}}\,d\Omega+\int_{\Gamma}\vec{\lambda}^T\left[\overline{E}_x+\overline{F}_y\right]\delta n d\Gamma\end{aligned} \tag{26}$$

In Eq. (26), the vectors $\vec{\lambda}$, and $\vec{\mu}$ can now be determined to eliminate the terms associated with $\delta\vec{\overline{Q}}$. Consequently, the costate (adjoint) equations are given as

$$-\overline{A}^T\vec{\lambda}_x-\overline{B}^T\vec{\lambda}_y=\vec{0} \qquad \text{in} \quad \Omega \tag{27}$$

Upon the combination of Eqs. (26) and (27), the variation of the functional becomes

$$\delta J_{\Gamma a} = \int_{\Gamma} \left\{ D_Q \delta \bar{\bar{Q}} + D_n \delta n + D\kappa \delta n + \vec{\mu}^T \left[\overline{H}_Q \delta \bar{\bar{Q}} + \overline{H}_n \delta n + \overline{H} \kappa \delta n \right] \right\} d\Gamma$$
$$+ \int_{\partial\Omega} \left\{ \vec{\lambda}^T \left[\overline{A} n_x + \overline{B} n_y \right] \delta \bar{\bar{Q}} \right\} d\Gamma + \int_{\Gamma} \vec{\lambda}^T \left[\overline{E}_x + \overline{F}_y \right] \delta n d\Gamma \tag{28}$$

With Eq. (A.11) in Appendix A of Ref. 32, we now express $\delta \bar{\bar{Q}}$ in terms of $\delta \vec{Q}$ to get

$$\delta \bar{\bar{Q}} = \delta \vec{Q} - \frac{\partial \vec{Q}}{\partial \vec{X}} \delta \vec{X} \tag{29}$$

For the sake of computational simplification, the variation of $\delta \vec{X}$ on the boundary is limited only to the y component in this study, i.e.,

$$\delta \vec{X} = \left[0, \delta y \right]^T \tag{30}$$

and Eq. (29) is simplified as

$$\delta \bar{\bar{Q}} = \delta \vec{Q} - \frac{\partial \vec{Q}}{\partial y} \delta y \tag{31}$$

Also an approximatation of Eq. (22) and use of Eq. (30), Eq. (22) can be written as

$$\delta n = \delta \vec{X} \circ \vec{n}$$

$$= \left[0, \delta y \right]^T \circ \left[n_x, n_y \right]$$

$$= n_y \circ \delta y \tag{32}$$

By use of Eqs. (29) - (32), Eq. (28) is now given as

$$\delta J_{\Gamma a} = \int_{\Gamma} \left\{ D_Q \delta \vec{Q} + n_y D_n \delta y + n_y D\kappa \delta y - n_y D_Q \vec{Q}_y \delta y + \right\} d\Gamma$$
$$+ \int_{\Gamma} \left\{ \vec{\mu}^T \left[\overline{H}_Q \delta \vec{Q} + n_y \overline{H}_n \delta y + n_y \overline{H} \kappa \delta y - n_y \overline{H}_Q \vec{Q}_y \delta y \right] \right\} d\Gamma$$
$$+ \int_{\Gamma} \left\{ \vec{\lambda}^T \left[\overline{A} n_x + \overline{B} n_y \right] (\delta \vec{Q} - n_y \vec{Q}_y \delta y) \right\} d\Gamma + \int_{\Gamma} \vec{\lambda}^T \left[\overline{E}_x + \overline{F}_y \right] n_y \delta y d\Gamma \qquad (33)$$

For arbitrary $\delta \vec{Q}$ and the variation of y on the boundary Γ, Eq. (33) gives the boundary conditions for the costate equations and the sensitivity equations, respectively, as

$$\left\{ \left[\overline{A} n_x + \overline{B} n_y \right]^T \vec{\lambda} + D_Q^T + \overline{H}_Q^T \vec{\mu} \right\} = \vec{0} \qquad \text{on } \Gamma \qquad (34)$$

and

$$\delta J_{\Gamma a} = \int_{\Gamma} \left\{ D_n + D\kappa - D_Q \vec{Q}_y + \vec{\mu}^T \left[\overline{H}_n + \overline{H} \kappa - \overline{H}_Q \vec{Q}_y \right] \right\} n_y \delta y d\Gamma$$
$$- \int_{\Gamma} \left\{ \vec{\lambda}^T \left[\overline{A} n_x + \overline{B} n_y \right] \vec{Q}_y \right\} n_y \delta y d\Gamma + \int_{\Gamma} \vec{\lambda}^T \left[\overline{E}_x + \overline{F}_y \right] n_y \delta y d\Gamma \qquad (35)$$

The unique determination of Eq. (35), therefore, demands the unique and converged solutions of Eqs.(9) and (10), (27), and (34).

2.2.3 Derivation of Constraint Sensitivity Equations

With the constraints defined in Eq. (13), the residual, and the boundary conditions, Eqs. (9) and (10), one can formulate the modified constraints as

$$G_{j\bar{\Gamma}a}\left(\vec{Q}, \vec{n}, \vec{\lambda}_j, \vec{\mu}_j \right) = \int_{\bar{\Gamma}} g_j \left(\vec{Q}, \vec{n} \right) d\bar{\Gamma} + \int_{\bar{\Omega}} \vec{\lambda}_j{}^T \left[\overline{E}_x + \overline{F}_y \right] d\bar{\Omega} + \int_{\bar{\Gamma}} \vec{\mu}_j{}^T \overline{H} \left(\vec{Q}, \vec{n} \right) d\bar{\Gamma}$$

$$\text{for } j = 1, 2, \ldots, \text{nconf} \qquad (36)$$

By following the same procedure as was done for the objective functional, the costate equations, boundary conditions, and the constraint derivative coefficients, respectively, can be expressed as

$$\left\{-\overline{A}^T\vec{\lambda}_{j_x} - \overline{B}^T\vec{\lambda}_{j_y}\right\} = \vec{0} \qquad \text{for } j = 1, 2, ..., \text{nconf} \qquad \text{in } \Omega \tag{37}$$

$$\left\{\left[\overline{A}n_x + \overline{B}n_y\right]^T\vec{\lambda}_j + g_{jQ}^T + \overline{H}_Q^T\vec{\mu}_j\right\} = \vec{0} \quad \text{for } j = 1, 2, ..., \text{nconf} \quad \text{on } \Gamma \tag{38}$$

$$\begin{aligned}\delta G_{j_{\Gamma a}} = &\int_\Gamma \left\{g_{j_n} + g_j\kappa - g_{jQ}\vec{Q}_y + \vec{\mu}_j^T\left[\overline{H}_n + \overline{H}\kappa - \overline{H}_Q\vec{Q}_y\right]\right\}n_y\delta y d\Gamma \\ &- \int_{\partial\Omega}\left\{\vec{\lambda}_j^T\left[\overline{A}n_x + \overline{B}n_y\right]\vec{Q}_y\right\}n_y\delta y d\Gamma + \int_\Gamma \vec{\lambda}_j^T\left[\overline{E}_x + \overline{F}_y\right]n_y\delta y d\Gamma \\ &\text{for } j = 1, 2, ..., \text{nconf}\end{aligned} \tag{39}$$

As can be discerned from Eq. (39), the computation of the constraint sensitivity equations requires the solution of a new set of costate equations and boundary conditions as many times as the number of constraints.

2.3 Numerical Optimization

Two steps are essentially followed in this approach. The first step is to determine the search direction, $\vec{S}$, and the second is to compute the magnitude of the step size α. These two quantities can be computed as proposed in Refs. 39 and 40 A typical computation of the feasible direction starts at the boundary of the feasible domain, and its magnitude and directions are kept constant as long as the search direction keeps the design variables in the feasible domain while improving the performance index. Otherwise, a new search direction and step size are recomputed with the new gradient information and this process continues until the optimality is met. Mathematically, the feasible direction can be formulated as

$$\vec{S}^T \circ \nabla g_i \le 0, \tag{40}$$

where i is part of the active constraints and the usable direction at a point is given by

$$\vec{S}^T \circ \nabla J_\Gamma \leq 0 \tag{41}$$

The change in design must be sought along the combination of the useable and feasible directions so that the functional or the performance index is reduced as much as possible, and the design is kept away from the constrained boundary as much as possible. By the use of Eqs. (40) and (41) in the method of feasible directions, the new design variables are updated as

$$\vec{X}_D^{n+1} = \vec{X}_D^n + \alpha \vec{S} \tag{42}$$

where n is the iteration number. The values of the design variables are continuously altered until the criteria for the optimal solution of the performance index are satisfied.

3. COSTATE EQUATIONS AND SOLUTION METHODS

3.1 Introduction to the Numerical Integration of Costate Equations

The coefficients of the costate equations are constant matrices whose components are derived from the converged solution of the state equations. They are globally constant in time and locally constant in space. But the interpretation of *constant* matrices must be understood in a sense that, during the time integration of the costate equations, only the costate variables evolve in space and time to convergence. The costate equations are identical to the Euler equations in form, but mathematically, they are different in the sense that they do not meet the homogeneity requirement to put them in a conservative form like the Euler equations. From the numerical view point, one can adopt any solution algorithm, which is used for the Euler equations, to the costate equations. This can be explained by the fact that the fluxes on the cell faces or at grid points can be artificially constructed by approximating the solution vector of the costate

equations either on the cell face from the right and left sides of the cell centers or at the grid points in exactly the same way one does for the state fluxes and solution vector.

The costate equations, like the state equations, are solved by use of the time dependent techniques. The Eqs. (27) and (37) are, therefore, modified to include the unsteady term with the proper signs so that this time dependent technique is fully exploited. Thus, for instance, Eq. (27) in the generalized coordinates system is expressed as

$$\pm\vec{\lambda}_\tau - \hat{A}^T\vec{\lambda}_\xi - \hat{B}^T\vec{\lambda}_\eta = \vec{0} \tag{43}$$

The proper sign selection of the time term is dependent on the complementary property of the well-posed boundary conditions of the state and costate equations. For Eq. (43) to be well-posed, the positive sign of the time term is selected, and Eq. (43) becomes

$$\vec{\lambda}_\tau - \hat{A}^T\vec{\lambda}_\xi - \hat{B}^T\vec{\lambda}_\eta = \vec{0} \tag{44}$$

3.2 Boundary (Transversality) Conditions

The objective functional boundary conditions, i.e. Eq. (34), in their general forms are again for the sake of convenience presented here as

$$\left\{\left[\overline{A}n_x + \overline{B}n_y\right]^T\vec{\lambda} + D_Q^T + \overline{H}_Q^T\vec{\mu}\right\} = \vec{0} \qquad \text{on } \Gamma \tag{45}$$

The objective functional and the no-mass penetration conditions are defined only on the solid boundary, and hence their derivative contributions in Eq. (45) are identically zero. Therefore, the boundary conditions for the inlet, exit, and center-line reduce to

$$\left\{\left[\overline{A}n_x + \overline{B}n_y\right]^T\vec{\lambda}\right\} = \vec{0} \qquad \text{on} \qquad (\Gamma_{inlet}, \Gamma_{center}, \Gamma_{exit}) \tag{46}$$

For the supersonic flow, the inlet condition is known, and hence the variation of the vector of the flow field is identically zero. Therefore, with Eq. (46), the values of the costate variables at the inlet boundary can be approximated from the internal stencils. Because the vector of the flow field is computed from the internal grids at the exit plane, Eq. (46) gives four linear independent equations for the costate variables, which result in all the costate varibles to be identically zero. On the centerline, the normal velocity is known to be zero, and one of the costate variables, for instance λ_3, is assigned a value, and the remaining flow field quantities are to be detemined from the resulting 3 x 3 system of equations as given in Eq. (45)

One way of treating the boundary conditions, i.e. Eq. (45), is to use Eq. (10) and to find a relationship between the conservative field variables $\vec{Q}$ by taking the variation of Eq. (10). This procedure eliminates the constant Lagrange multipliers $\vec{\mu}$ and modifies the functional sensitivity derivatives, Eqs. (35) and (39) by a term resulting from the variation of the normal vector $\vec{n}$ at the solid boundary.

On the solid boundary, on the other hand, the costate variables are determined by use of the complete form of the compatibility relationships and the sign of the eigenvalues of the costate Jacobian matrices. Once the values of the costate variables on the solid boundary are computed, the constant Lagrange multipliers $\vec{\mu}$ of the no-mass penetration condition can be calculated by solving the complete set of the boundary condition. The results presented in this study are obtained by solution of the complete boundary conditions as given in Eqs. (34) and (38).

3.3 Linearization of Costate (Adjoint) Equations

By the same linearization procedure we used for the state equations, Eq. (44) can be approximated as follows:

$$\vec{\lambda}_\tau - \Delta\tau \frac{\partial}{\partial\tau}\left\{\hat{A}^T\vec{\lambda}_\xi + \hat{B}^T\vec{\lambda}_\eta\right\} = \left\{\hat{A}^T\vec{\lambda}_\xi + \hat{B}^T\vec{\lambda}_\eta\right\}^n \tag{47}$$

$$\vec{\lambda}_\tau - \Delta\tau \frac{\partial}{\partial\tau}\left\{\left[\hat{A}^T\delta_\xi + \hat{B}^T\delta_\eta\right]\vec{\lambda}\right\} = \left\{\hat{A}^T\vec{\lambda}_\xi + \hat{B}^T\vec{\lambda}_\eta\right\}^n \tag{48}$$

$$\vec{\lambda}_\tau - \Delta\tau \frac{\partial}{\partial \lambda}\left\{\left[\hat{A}^T\delta_\xi + \hat{B}^T\delta_\eta\right]\vec{\lambda}\right\}\frac{\partial\vec{\lambda}}{\partial\tau} = \left\{\hat{A}^T\vec{\lambda}_\xi + \hat{B}^T\vec{\lambda}_\eta\right\}^n \tag{49}$$

By approximation of the time and space terms, Eq. (49) becomes

$$\Delta\vec{\lambda}^n - \Delta\tau\left[\hat{A}^T\delta_\xi + \hat{B}^T\delta_\eta\right]\Delta\vec{\lambda}^n = \Delta\tau\left\{\left[\hat{A}^T\delta_\xi + \hat{B}^T\delta_\eta\right]\vec{\lambda}\right\}^n \tag{50}$$

3.4 Time-Integration Method

In this study we have used the implicit, i.e., the ADI method to drive costate equations to steady state. For the implicit method, the ADI factorization of Eq. (50) is used to split it into the ξ and η sweeps. Let us define the right side R_λ of Eq. (50) as

$$R_\lambda = \Delta\tau\left\{\left[(\hat{A}^-)^T\delta_\xi^+ + (\hat{A}^+)^T\delta_\xi^- + (\hat{B}^-)^T\delta_\eta^+ + (\hat{B}^+)^T\delta_\eta^-\right]\vec{\lambda}\right\}^n \tag{51}$$

where R_λ is the residual for the costate equations. Also, Eq. (50) can be put in its split form of Jacobians and fluxes as

$$\left\{I - \Delta\tau\left[(\hat{A}^+)^T\delta_\xi^- + (\hat{A}^-)^T\delta_\xi^+ + (\hat{B}^+)^T\delta_\eta^- + (\hat{B}^-)^T\delta_\eta^+\right]\right\}\Delta\vec{\lambda}^{n^*} = R_\lambda \tag{52}$$

Then the ξ and η sweeps of Eq. (52) are given as

$$\left\{I - \Delta\tau\left[(\hat{A}^+)^T\delta_\xi^- + (\hat{A}^-)^T\delta_\xi^+\right]\right\}\Delta\vec{\lambda}^{n^*} = R_\lambda \tag{53}$$

and

$$\left\{I - \Delta\tau\left[(\hat{B}^+)^T\delta_\eta^- + (\hat{B}^-)^T\delta_\eta^+\right]\right\}\Delta\vec{\lambda}^n = \Delta\vec{\lambda}^{n^*} \tag{54}$$

4. RESULTS AND DISCUSSION ON DESIGN OPTIMIZATION OF INTERNAL FLOWS USING TW0-DIMENSIONAL EULER EQUATIONS

The main thrust of this section is to briefly discuss the the numerical results of the variational sensitivity analysis that are obtained by the use of two-dimensional Euler flow equations. Additionally, the efficiency and accuracy of the variational sensitivity in comparison to the finite difference are analyzed.

4.1 Two-Dimensional Nozzle Optimization Problem Formulation

At least a couple of reasons can be given for choosing the two-dimensional nozzle geometry in order to demonstrate our point of optimization methodology. The first one is that one can easily obtain various types of nozzle geometries by simply using already known analytical expressions for different flow conditions. The second important reason is also the need to develop a scramjet nozzle afterbody for the High-Speed Civil Transport. The third one is the need to develop efficient wind tunnels with optimal shapes for various experimental wind tunnel applications. The optimization problem demonstrated here seeks the optimal shape for the maximum thrust in conjunction with the nonreverse flow condition at the exit. Hence, the example problem is formulated as the maximization of the functional defined by

$$J_{\bar{\Gamma}} = \int_{\bar{\Gamma}} P d\bar{\Gamma} \tag{55}$$

with the constraint that the static pressure P at the exit assumes a certain percentage of the ambient pressure p_∞ for maximum expansion at that exit lip of the solid boundary. Therefore, the constraint is mathematically posed as

$$G_j(\vec{Q},\vec{n}) = \int_{\bar{\Gamma}} \left[(1 - \frac{p}{p_\infty}) + \left| 1 - \frac{p}{p_\infty} \right| \right] d\bar{\Gamma} \le 0 \tag{56}$$

4.2 Two-Dimensional Nozzle Flow

The initial geometry for this internal flow configuration is given in Fig. 1. It is a supersonic nozzle where only half of the physical domain is considered with 137 x 69 grid points. It is a convex type of geometry with the smallest area at the inlet and a diverging afterbody for supersonic expansion. The only aerodynamic inequality constraint considered is the criteria on the static pressure at the exit lip of the nozzle to reach a certain percentage of the ambient pressure as a necessary condition to avoid any reverse flow from underexpansion as the shape evolves during the optimization cycle.

To assess the variational methods for sensitivity analysis, computational efficiency and accuracy calculated by variational methods and finite difference are compared. One of the obvious limitations with the finite difference is the uncertainty to *a priori* determine the step size that will give reliable sensitivity derivatives. The magnitude of the stepsize is dependent on how accurate one needs the derivatives to be. If, for instance, one only needs a 10% deviation from the assumed exact derivative, then the step size must be under a 10% range of the derivative. In our case of computing the sensitivity derivatives using the finite difference, we have assigned the step size to be 0.0001.

The x component of the design variables (Bezier control points) are *a priori* computed as being spatially invariable, and the variation of the design variables is allowed only in the y direction. This apparent limitation of the design variables must not be a hindrance since addition or deletion of any desired design variables in the design domain will produce the same result. To verify this claim, two sets of design variables, in addition to the assumed optimal number of design variables (in this case the optimum is eight design variables), were investigated. The first set was performed by increasing the number of design variables by four and the second one by decreasing it by four from the optimal number of design variables. Here, the optimal number defined as that number of design variables which reproduces the closest shape to that of the initial geometry.

As presented in Table 1, the CPU time and memory requirements of complete cycle of optimization for the two additional sets of design variables are almost identical for the two-dimensional optimization case. Therefore, the eight design variables are considered as the optimal number of design variables which produced the desired computational efficiency for our test case. On the other hand, this slight memory increase as the number of design variables increases could be a warning to the eventual computational memory increase as the dimensionality, number of constraints, and design variables increase. The second aspect of the role played by the number of design variables may be the influence on the optimal shape (Fig. 2). All three categories of the design variables produced slightly different optimum shapes from each other. Comparing all three shapes (Fig. 2), the shape produced by twelve design variables appears to follow the shape produced by the four design variables in the compression area (upstream) and the shape of the eight design variables in the expansion area (downstream). The shape generated by the optimal number of eight design variables shows a slight change of shape upstream, from approximately x=0.1 to x=0.375, and downstream, from approximately x = 0.7 to x = 1.0 as compared with the shapes generated by the other sets of design variables. The shape change in the compression area seems to be more desirable beause it produces high-pressure ratios and thereby gives more thrust as one integrates the change of pressure along the changing nozzle shape. The shape change in the expansion region, on the other hand, reduces the ratio of the static pressure to the ambient pressure, which results in less thrust augmentation. This physical phenomena is further reflected in Fig. 3 where the optimal thrust of the eighth design variable shape is higher than the other two design variable shapes.

From the parametric studies (four, eight, and twelve design variables) conducted, one may conclude that the eight design variables are the *optimal* number of design variables to sufficiently represent the nozzle shape and at the same time to give a better thrust and computational efficiency.

The evolution of the design variables for the variational methods and the finite difference approach are given in Figs. 4 and 5, respectively. Except for the second and the seventh design

variables, the general trend of the evolution of the design variables in both approaches is similar. In the variational case, the second design variable approaches the first design variable and the seventh one tends to come close to the eighth design variable. In the finite difference case, however, the second and the seventh design variables tend to pull away from the first and eighth design variables, respectively. As shown in Fig. 6, due to the movement of the second and the seventh design variables in the opposite direction, the optimal shapes of the variational methods and finite difference are slightly different. As explained in the parametric studies, the decrease of the optimal (as compared with the initial) shape or optimal design variables in the compression region is much more advantageous to the decrease of the optimal shape or optimal design variables in the expansion region for the supersonic flow regime. This is due to the effect that the decrease of the shape in the upstream results in the substantial gain of high pressure ratio (compare Figs. 7 and 8) which favors the augmentation of more thrust (Fig. 9) in the design process. Figure 9 also clearly indicates that the pressure distribution in the expansion region in general and at the lip of the nozzle in particular is within the constraint specification as imposed in the aerodynamical constraint given by Eq. (56).

As given in Table 2, the accuracy of the variational methods is verified by comparing the variational functional sensitivity derivatives to the functional derivatives of finite difference. If one takes into consideration that the sensitivity coefficients of the finite difference are dependent on the step sizes, then the gradient values obtained by the variational methods are well within the engineering prediction range, except for the second and the seventh sensitivity coefficients. The discrepancy of those two sensitivity values may be associated with the difficulty to properly implement the boundary conditions of the adjoint equations. Despite the differences on these two sensitivity derivatives which correspond to the second and seventh design variables, the optimal shape and thrust of the variational methods are comparable with those of the finite difference as presented in Table 3 and Fig. 6. It is known that the finite difference uses function evaluations to compute the gradient information while the variational methods solve another set of partial differential equations and sensitivity derivative equations. Due to this, there is a memory

increment of approximately 1.3 mega words as shown in Table 4. This slight increment in memory is negligible as compared with the other gradient-based sensitivity analysis approaches, such as the discrete sensitivity analysis which requires higher memory allocation for the given optimization problem.

5. CONCLUSIONS

A two-dimensional nozzle optimization problem was considered, and the application of variational methods to compute the optimal shape for the maximum thrust is presented. During the design process, the supersonic nozzle remained supersonic while improving the performance index or thrust (Table 2). Also, while the VM's computational accuracy (Table 3) is comparable with the finite difference, its computational efficiency and memory savings (Table 4) are found to be substantial. As memory and computational efficiency are the bottle-necks for large two-dimensional and three-dimensional problem in general, variational methods are one of the most viable candidates in solving design optimization problems.

REFERENCES

1. Abbott, I. H., and Von Doenhoff, A. E., *Theory of Wing Sections, Including a Summary of Airfoil Data*, Dover Publications, Inc., New York, 1959.

2. Whitcomb, R. T., "Review of NASA Supercritical Airfoils," *9th Congress of the International Council of Aeronautical Sciences* (ICAS), Haifa, Israel, ICAS Paper 74-10, August 1974.

3. Valarezo, W. O., Dominik, C. J., McGhee, R. J., Goodman, and W. L., Paschal, K. B., "Multi-Element Optimization for Maximum Lift at High Reynolds Numbers," *AIAA Applied Aerodynamics Conference, 9th, Baltimore, MD*, AIAA-91-3332-CP, September 1991.

4. Huddleston, D. H., and Mastin, C. W., "Optimization of Aerodynamic Designs Using Computational Fluid Dynamics," AGARD-CP-463, Paper No. 23, May 1989.

5. Vanderplaats, G. N., "ADS - A Fortran Program for Automated Design Synthesis," Version 1.10, NASA Contractor Report 177985, September 1985.

6. Hicks, R. M., Murman, E. M., and Vanderplaats, G. N., "An Assessment of Airfoil Design By Numerical Optimization," NASA TM X-3092, July 1974.

7. Vanderplaats, G. N., "Approximation Concepts for Numerical Airfoil Optimization," NASA TP-1370, March 1979.

8. Vanderplaats, G. N., "An Efficient Algorithm for Numerical Airfoil Optimization," AIAA Paper No. 79-0079, January 1979.

9. Pittman, J. L., "Supersonic Airfoil Optimization," *Journal of Aircraft*, Vol. 24, No. 12, December 1987, pp. 873 - 879.

10. Elbanna, H. and Carlson, L., "Determination of Aerodynamic Sensitivity Coefficients in the Transonic and Supersonic Regimes'" *Journal of Aircraft*, Vol. 27, No. 6, June 1990, pp. 507 - 518.

11. Eleshaky, M. E., "A Computational Aerodynamic Design Optimization Method Using Sensitivity Analysis," Ph.D. Dissertation, Old Dominion University, May 1992.

12. Burgreen, W. G., "Three Dimensional Aerodynamic Shape Optimization Using Discrete Sensitivity Analysis," Ph.D. Dissertation, Old Dominion University, May 1994.

13. Taylor, A. C, III, Hou, G. J.-W., and Korivi, V. M., "Sensitivity Analysis, Approximate Analysis, and Design Optimization for Internal and External Viscous Flows," AIAA Paper 91-3083, September 1991.

14. Newman, P. A., Hou, G. J.-W., Jones, H. E., Taylor, A. C., III, and Korovi, V. M., "Observations on Computational Methodologies for Use In Large-Scale Gradient-Based Multi-disciplinary Design," *Proceedings of the Fourth AIAA/USAF/NASA/OAI Symposium on Multidisciplinary Analysis and Optimization*", AIAA, Cleveland, OH, September 1992, pp. 531 - 542.

15. Hou, G. J-W., Taylor , C. A., III, Korivi, M. V., "Discrete Shape Sensitivity Equations for Aerodynamic Problems," AIAA-91-2259, AIAA/SAE/ASME/ASEE 27th Joint Propulsion Conference, June 24-27, 1991.

16. Pironneau, O., "On Optimum Profile in Stokes Flow," *Journal of Fluid Mechanics*, Vol. 59, Part 1, June 1973, pp. 117 - 128.

17. Chen, W H., and Sienfeld, J. H., "Estimation of the Location of the Boundary of a Petroleum Reservoir," *Society of Petroleum Engineers Journal,* Vol. 15, No. 1, February 1975, pp. 19 - 38.

18. Koda, M., Dogru, A. H., and Sienfeld, J. H., "Sensitivity Analysis of Partial Differential Equations with Application to Reaction and Diffusion Process," *Journal of Computational Physics*, Vol. 30, No. 2, February 1979, pp. 259 - 282.

19. Koda, M., "Sensitivity Analysis of the Atmospheric Diffusion Equations," *Atmospheric Environment*, Vol. 16, No. 11, November 1982, pp. 2595 - 2601.

20. Koda, M., " Optimum Design in Fluid Mechanical Distributed-Parameter Systems," *Large Scale Systems*, Vol. 6, No. 3, June 1984, pp. 279 - 291.

21. Koda, M., "Sensitivity Analysis of Descriptor Distributed Parameter Systems," *International Journal of System Science*, Vol. 19, No. 10, October 1988, pp. 2103 - 2114.

22. Meric, R. A., "Finite Element Analysis of Optimal Heating of Slab with Temperature Dependent Thermal Conductivity," *International Journal Heat and Mass Transfer*, Vol. 22, No. 10, October 1979, pp. 1347 - 1353

23. Meric, R. A., "Boundary Element Methods for the Optimization of Distributed Parameter Systems," *International Journal for Numerical Methods in Engineering*, Vol. 20, July 1984, pp. 1291 - 1304.

24. Shubin, G. R. , and Frank, P. D., "A Comparison of the Implicit Gradient Approach and the Variational Approach to Aerodynamic Design Optimization," Boeing Computer Services, April 1991.

25. Jameson, A., "Aerodynamic Design via Control Theory," ICASE, NASA Langley Research Center, ICASE Report No. 88-64, November 1988.

26. Cabuk, H., Modi, V., "Optimum Plane Diffusers in Laminar Flow," *Journal of Fluid Mechanics*, Vol. 237, April 1992, pp. 373 - 393.

27. Ta'asan, S., Kuruvilla, K. and Salas, M. D., "Aerodynamic Design and Optimization in One Shot," AIAA 92-0025, January 1992.

28. Ibrahim, A. H., and Baysal, O., "Design Optimization Using Variational Methods and CFD," AIAA-94-0093, January 1994.

29. Reuter, J., and Jameson, A., "Control Theory Based Airfoil Design for Potential Flow and Finite Volume Discretization," AIAA 94-0499, January 1994.

30 Iollo, A., and Salas, D. M., "Contribution to the Optimal Shape Design of Two-Dimensional Internal Flows With Embedded Shocks," ICASE, NASA Langley Research Center, ICASE Report No. 95-20, March 1995.

31. Borggaard, J. T., "On the Presence of Shocks in Domain Optimization of Euler Equations," *IMA Workshop on Flow Control*, Institute for Mathematics and its Application, University of Minnesota, Minneapolis, November 1992.

32. Ibrahim, A. H., "Variational Methods in Sensitivity Analysis and Optimization for Aerodynamic Applications," Ph.D. Dissertation, Old Dominion University, May 1996.

33. Thibert, J. J., "One Point and Multipoint Design Optimzation for Airplane and Helicopter Application," *Special Course on Inverse Methods for Airfoil Design for Aeronautical and Turbomachinery Applications*, AGARD-R-780, Paper No. 10, November 1990.

34. Mortenson, E. M., *Geometric Modeling*, John Wiley & Sons, 1985.

35. Smith, R. E., and Kerr, P. E., "Geometric Requirements for Multidisciplinary Analysis of Aerospace-Vehicle Design," *4th, AIAA-USAF-NASA-OIA Symposium on Multidisciplinary Analysis and Optimization*, AIAA-92-4773, Cleveland, Ohio, September 1992.

36. Gelfand, I. M., and Fomin, S. V., *Calculus of Variations*, Prentice-hall, Inc, 1963.

37. Haug, E. I., Choi, K. K., and Komkov, V., *Design Sensitivity Analysis of Structural Systems*, Academic Press, Inc, 1986.

38. Pironneau, O., *Optimum Shape Design for Elliptic Systems*, Springer-Verlag, 1984.

39 Vanderplaats, G. N., and Moses, F. "Structural Optimization by Methods of Feasible Directions," *Computers and Structures*, Vol. 3, July 1973, pp. 739 - 755.

40. Haftka, R. T., and Gurdal, Z., *Elements of Structural Optimization*, Third Revised and Expanded Edition, Kluwer Academic Publishers, 1991.

Table 1. CPU Time and Memory for Four, Eight, and Twelve Design Variables With Variational Methods

Design variables	CPU time (sec)	Memory (MGW)
4	868.0463	5.249459
8	864.2226	5.249939
12	866.2128	5.250579

Table 2. Sensitivity Derivatives by Variational Methods and Finite Difference

X_D	Variational methods	Finite difference	Deviation (%)
1	9.1483E-2	9.4441E-2	3.1
2	7.9228E-2	1.1062E-2	86.0
3	-6.6563E-2	-4.7906E-2	28.1
4	-5.5491E-2	-5.9409E-2	6.6
5	-4.6421E-2	-5.3278E-2	12.9
6	-3.8979E-2	-4.6287E-2	15.8
7	-3.2186E-2	-6.9988E-2	53.9

Table 3. Initial and Optimal Values of Functional and Constraint for Variational Methods and Finite Difference

		Variational methods	Finite difference
Initial	Functional	0.045481	0.045481
	Constraint	- 2.10787	-2.10787
Optimum	Functional	0.049958	0.049885
	Constraint	-0.5858	-0.5668

Table 4. Efficiency Comparison Between Variational Methods and Finite Difference

			Variational methods	Finite difference
CPU time (sec)	Complete optimization		865.098	4356.33
	Single analysis	Euler equations		128.23
		Co-state equations	58.59	
Memory (MGW)	Complete optimization		5.25 (with sensitivity eqs.)	3.98 (no sensitivity eqs.)

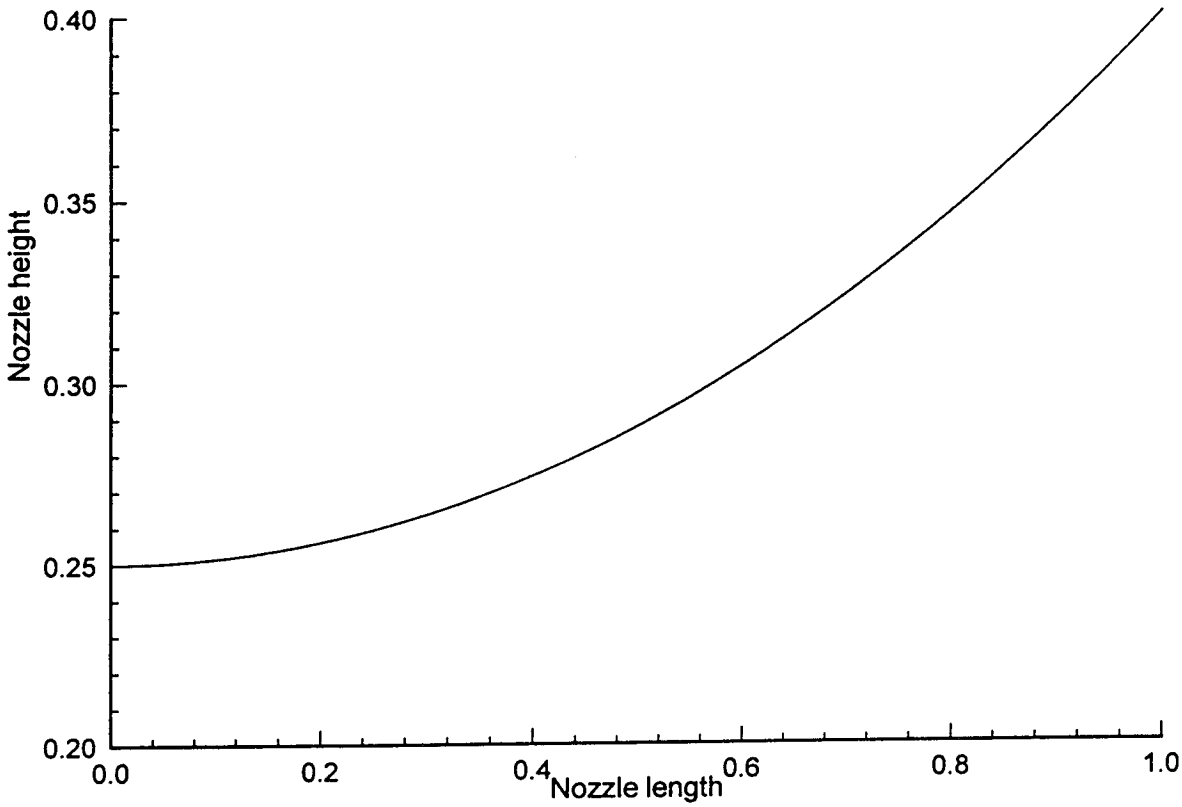

Fig. 1 Initial supersonic nozzle shape.

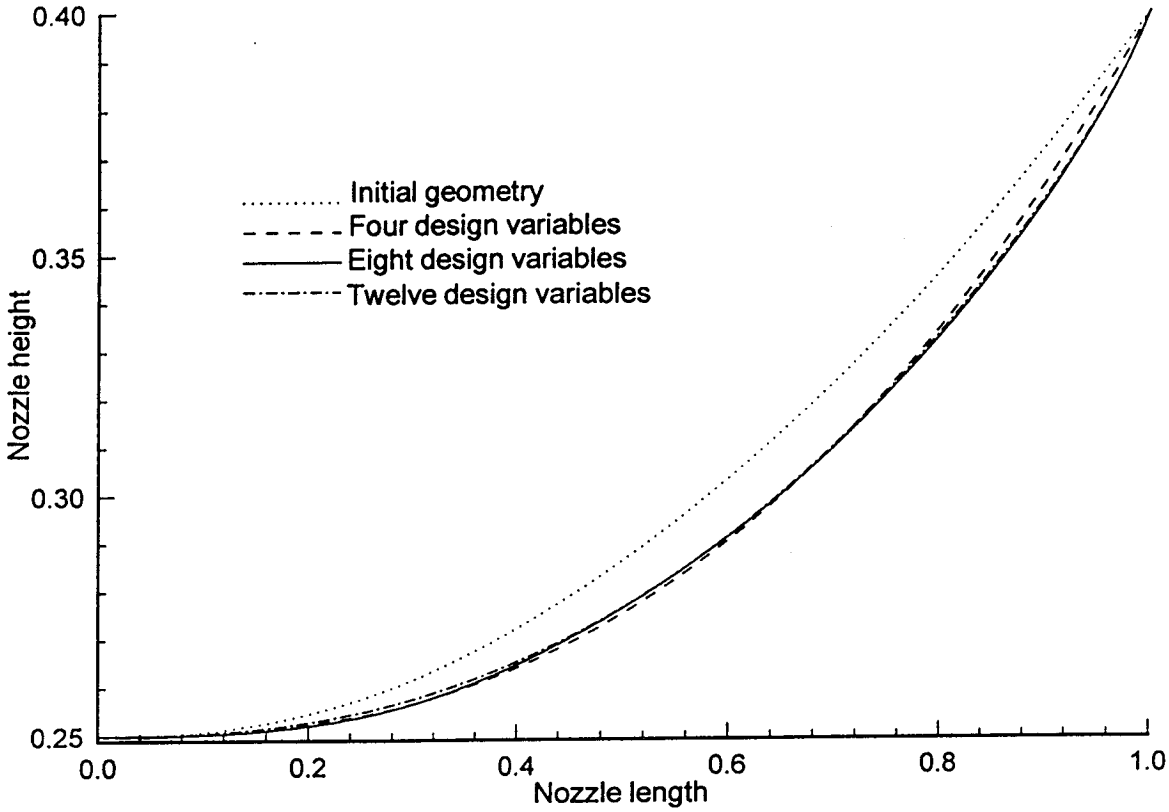

Fig. 2 Effect of the number of design variables on the optimal shape.

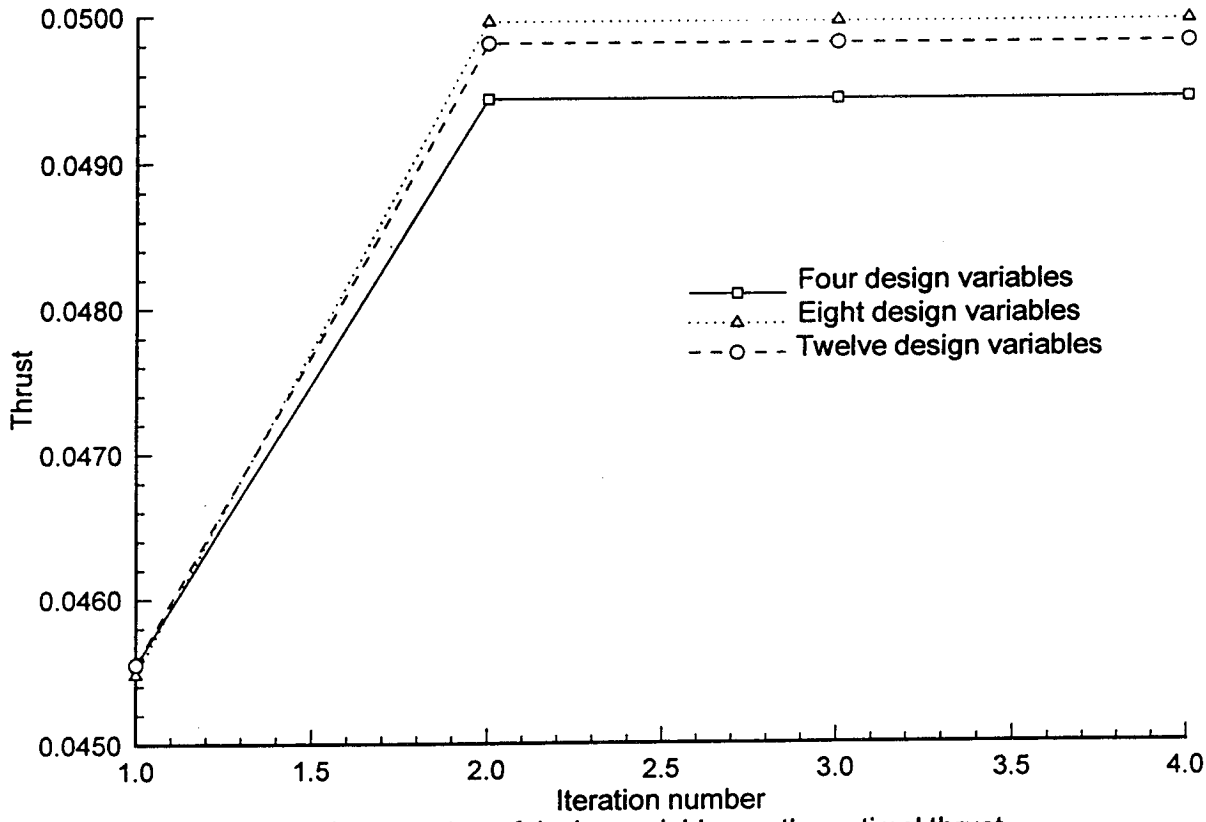

Fig. 3 Effect of the number of design variables on the optimal thrust.

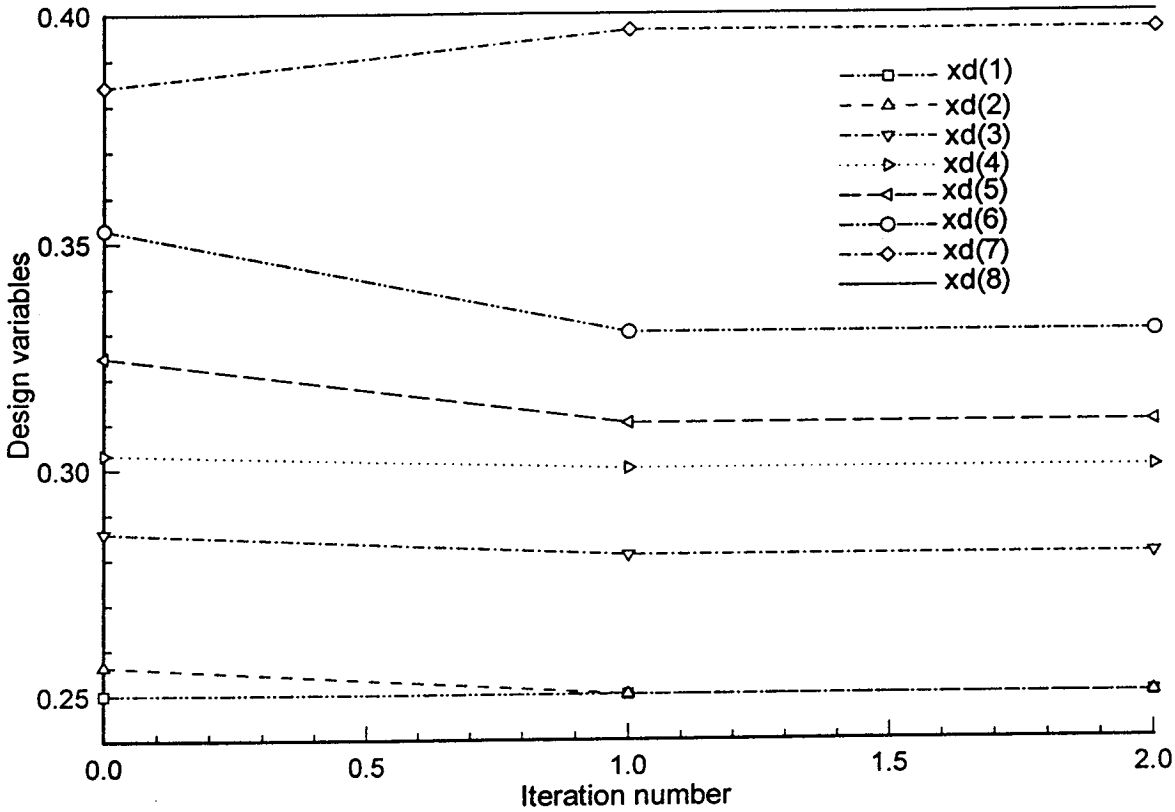

Fig. 4 History of the design variables for the variational methods.

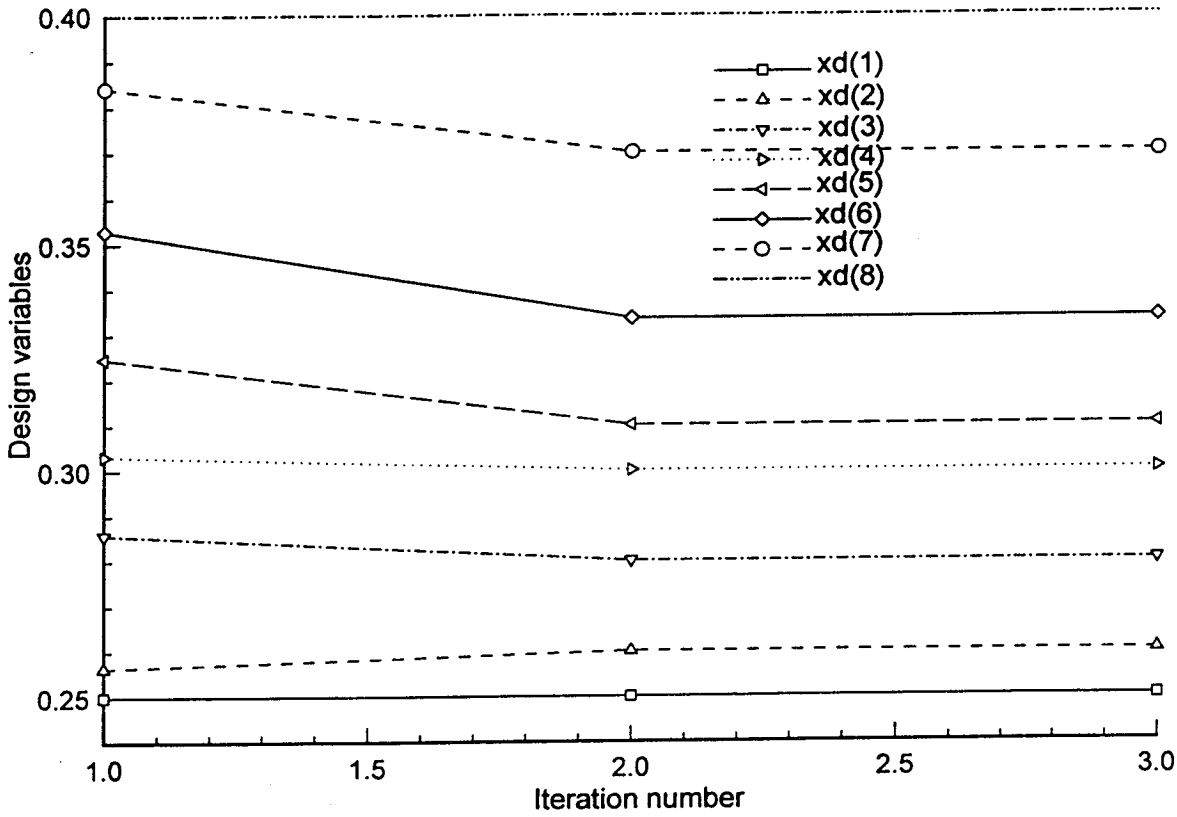

Fig. 5 History of the design variables for the finite difference.

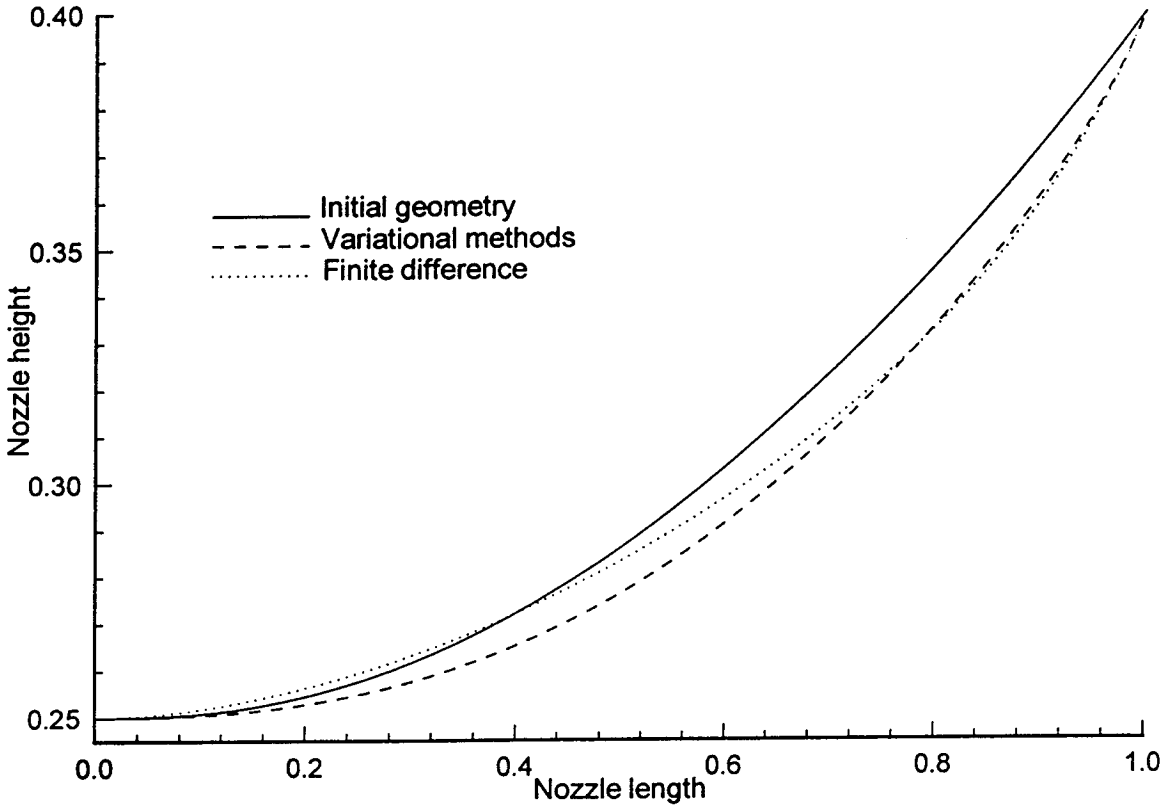

Fig. 6 Optimal shapes by variational methods and finite difference.

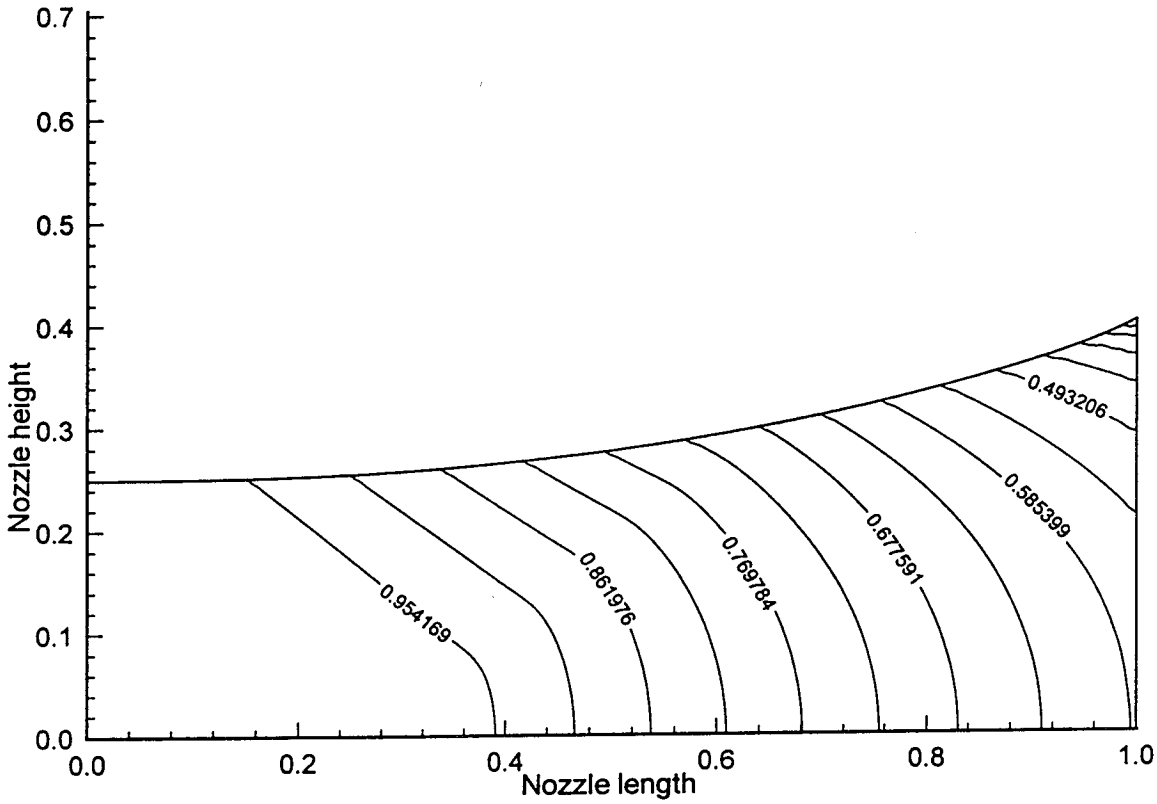

Fig. 7 Optimal pressure countour by variational methods.

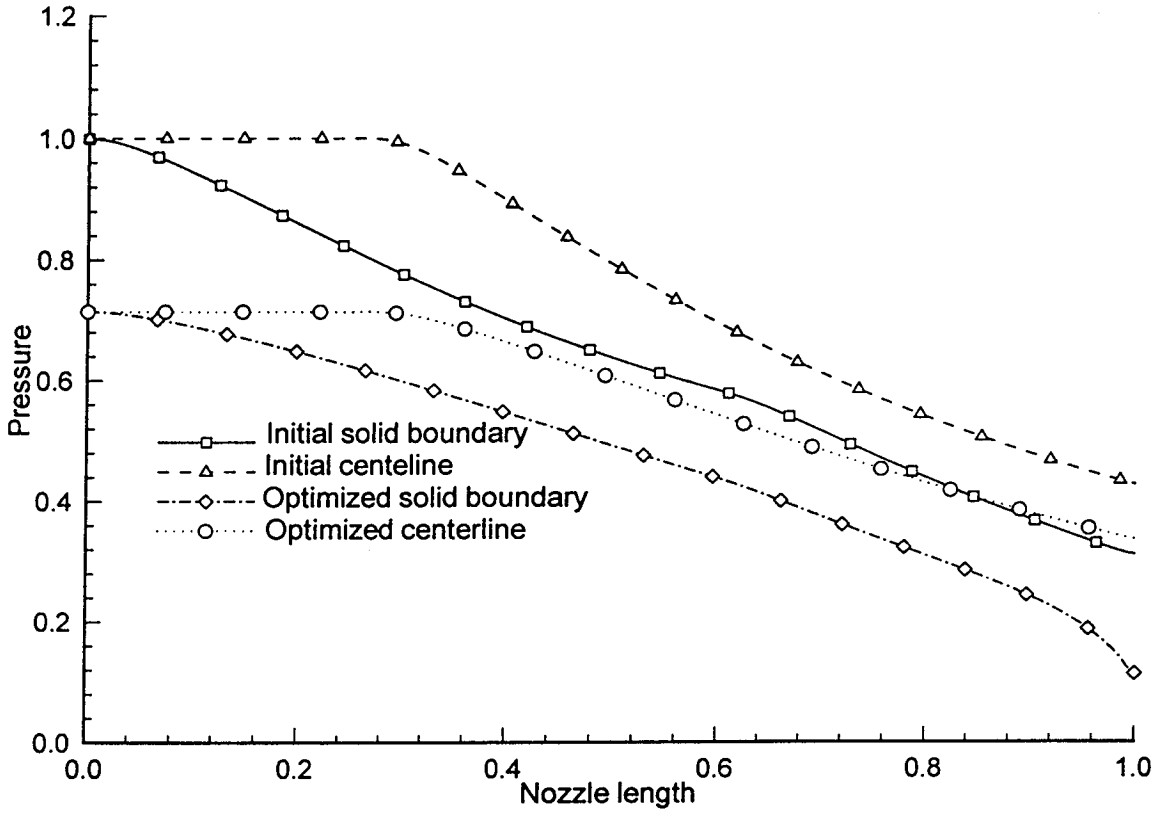

Fig. 8 Pressure distributions on the solid and symmetry line by variational methods.

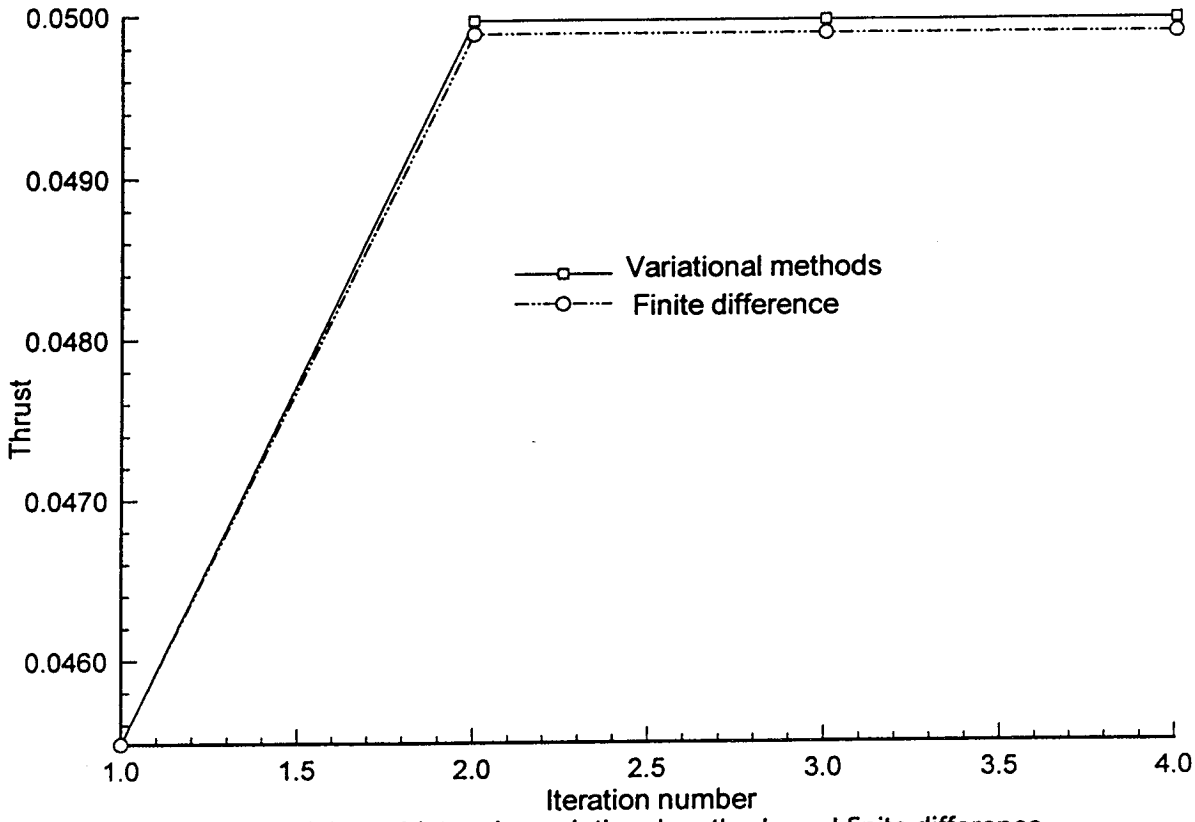

Fig. 9 Optimal thrust history by variational methods and finite difference.